Corrosion Protection of Mild Steel by a New Phosphonated Pyridines Inhibitor System in HCl Solution

Lilia Tabti, Redha Khelladi, Nadjib Chafai, Alexandre Lecointre, Aline Nonat, Loic Charbonnière, Embarek Bentouhami

Published in "Advances Engineering Forum

Corrosion protection of mild steel by a new phosphonated Pyridines inhibitor system in HCl solution

Lilia Tabti[a], , Redha.M. Khelladi[a,b], Nadjib Chafai[c] , Alexandre Lecointre[d], Aline M. Nonat[d] and Loic J. Charbonnière[d], Embarek Bentouhami[a*].

[a]LCIMN, Laboratory, Department of Process Engineering, Faculty of Technology, University Ferhat Abbas Setif -1, 19000 Sétif, Algeria

[b]Department of Materials Science, Faculty of Sciences and Technology, Mohamed El Bachir El Ibrahimi University, Bordj-Bou-Arreridj 34030, Algeria

[c]LEMMC, Laboratory, Department of Process Engineering, Faculty of Technology, University Ferhat Abbas Setif -1, 19000 Sétif, Algeria

[d]LIMAA, IPHC, UMR 7178, University de Starsbourg, ECPM, 25 rue Becquerel, 67087 Strasbourg Cedex 02, France

Corresponding author. E-mail address: **labunivstrasbg@gmail.com**

Abstract

The adsorption behavior and inhibition mechanism of (1, 4, 7-Tris [hydrogen (6-methylpyridin-2-yl) phosphonate] -1, 4, 7-triazacyclononane) (TPP) on the corrosion of mild steel in 1 M HCl were investigated by weight loss technique, potentiodynamic polarization, and electrochemical impedance spectroscopy (EIS) methods for different concentrations at 25°C. The results show that the inhibition efficiency values depend on the amount of immersion times and the concentration. A 90% efficiency is found at the highest concentration of the studied compound according to weight loss measurements. The adsorption of the investigated inhibitor on the mild steel surface was well supported using an AFM study. For the assignment of the absorption sites, we performed quantum chemical calculations with (DFT) method. The interaction between the inhibitor and iron surface were performed by molecular dynamic (MD) simulations. In this paper, experimental methods and results used to assess the efficiency of the studied compound are presented.

***Keywords*:** Phosphonated Pyridines; TPP; Inhibitor; Cyclic voltammetry; DFT calculations.

1. Introduction

Mild steel is widely used as a structural material in automobiles, pipes and chemical industries [1], it undergoes severe corrosion in pickling processes. Hydrochloric and sulfuric acids are widely used for the pickling and the de-scaling of mild steel [2–4]. The use of organic inhibitors is one of the most practical methods and cost-effective choices for protecting metals against corrosion. These organic inhibitors are usually adsorbed on the metal surface via formation of a coordinate covalent bond (chemical adsorption) or the electrostatic interaction between the metal and inhibitor (physical adsorption) [5]. This adsorption produces a uniform film, which isolates the metal surface from the aggressive medium and consequently reduces the corrosion extent [6]. The extent of adsorption depends on the electronic and structural characteristics of the inhibitor, the nature of the surface, the temperature and the pressure of the reaction, the flow velocity as well as the composition of the aggressive environment [7–12]. In general, organic inhibitors containing triple or conjugated double bonds, or aromatic rings in their molecular structures, and those rich in heteroatoms such as sulfur, phosphorus, nitrogen and oxygen were found to be highly electronegative and having electron donating ability; this increases the inhibition efficiency of these compounds in acidic media [13–15]. The implementation of phosphonic acids for the protection of iron and its alloys from corrosion in different media have been the subject of several research works [16- 20].

In this paper, we report a new organic inhibitor (1,4,7-tris[hydrogen (6-methylpyridin-2-yl) phosphonate]-1,4,7-triazacyclononane) (TPP) [21]. To our knowledge, TPP has not been considered as a corrosion inhibitor. TPP is chosen as a such mainly based on the following factors: the first is that it contains multiples N, P and O as active centers and a pyridine rings system. Secondly, it has a high solubility in acidic media. The inhibition effect of the TPP on the corrosion of mild steel XC48 in hydrochloric acid using the gravimetric and electrochemical techniques such as potentiodynamic polarization and impedance measurements. On an other hand, the surface state of the mild steel specimens was observed by using atomic force microscopy (AFM). Theoretical studies on electronic and molecular structures were conducted using quantum chemical calculations. Finally, MD simulations studies are used to discuss the adsorption configuration, adsorption energy and explain the mechanism of TPP on iron (110) surface.

2. Experimental

2.1. Inhibitor

(1, 4, 7-tris [hydrogen (6-methylpyridin-2-yl) phosphonate]-1, 4, 7-triazacyclononane)(**TPP**) was synthesized from tacn (325 mg, 2.5 mmol), and flame-dried K_2CO_3 according to literature [21].The chemical structure of the compound is given in Fig. 1.

2.2. Electrolytic Solution

The aggressive solution electrolyte grad of 37%M HCl was prepared by dilution with distilled water. The concentrations of the inhibitors **TPP** was varied from 0.010 mM to 0.075mM.

2.3. Gravimetric Measurements

Steel specimens of a dimension of 2 cm, 0.7 cm respectively cleaned with emery papers (having different grades), washed several times with distilled water, acetone then dried in desiccator. The specimens were immersed in 50 mL of 1 M HCl for 40 h in both the absence and the presence of different concentrations of the inhibitor **TPP**. After an amount of time, the specimens were taken out, washed and weighted. The experiment was performed three times, from gravimetric measurements, [22, 23] the corrosion rate (A), the surface coverage (θ) and inhibition efficiency ($\eta_w\%$) follows the following equations:

$$A = \frac{\Delta W}{St} = \frac{W_1 - W_2}{S \times t} \qquad (1)$$

$$\theta = \frac{A^{\circ}_{corr} - A_{corr}}{A^{\circ}_{corr}} \qquad (2)$$

$$\eta_w\% = \frac{A^{\circ}_{corr} - A_{corr}}{A^{\circ}_{corr}} \times 100 \qquad (3)$$

W_1 and W_2 are respectively the weight of specimens before and after plunge in the examined solution, ΔW is the average weight loss (mg). S is the total area of the specimen (cm^2), t is the corrosion time (h), A°_{corr} and A_{corr} are corrosion rates in the absence and presence of the inhibitor, respectively.

2.4. Electrochemical Measurements

Electrochemical measurements such as Tafel polarization and electrochemical impedance were conducted on a (PGZ 301 voltalab40 model potentiostat/galvanostat) system connected to a computer. The electrochemical cell consists of an ordinary three-electrode with platinum as a counter electrode, saturated calomel electrode (SCE) as a reference electrode and a mild steel specimen as a working electrode.

The mild steel specimens was exposed to 1M HCl corrosive medium in the absence and presence of different concentrations of inhibitor for 1h before starting the electrochemical experiments at room temperature and under an open circuit potential (OCP) to reach a steady-state The impedance experiments (EIS) were carried out from Nyquist plot using alternating current (AC) signal of 0.01 V amplitude for the frequency spectrum from 100 kHz to 0.01 Hz. [24] The values of inhibition efficiency is calculated from charge transfer resistances was obtained using the following equation :

$$E_R\% = \frac{R_{t(inh)} - R_{t(0)}}{R_{t(inh)}} \times 100 \qquad (4)$$

$R_{t(0))}$ and $R_{t(inh)}$ are respectively the charge transfer resistances in the absence and presence of the inhibitor.

Tafel plots were registered after the impedance measurement by polarizing the specimen from -700 to -250 (mV/SCE) at a scan rate 2 mV/s. [25, 26] the inhibitory efficiency $E_P\%$ and the surface coverage (θ) are determined by the following equations.

i°_{corr} and $\mathrm{i_{corr\,(inh)}}$ correspond to the corrosion current density in the absence and in the presence of inhibitor respectively.

$$\mathrm{E_P\%} = \frac{\mathrm{i^{\circ}_{corr} - i_{corr(inh)}}}{\mathrm{icorr}} \times 100 \qquad (5)$$

$$\theta = \frac{\mathrm{i^{\circ}_{corr} - i_{corr(inh)}}}{\mathrm{icorr}} (6)$$

2.5. Surface studies

The surface morphology of an immersed mild steel specimen in 1 M hydrochloric acid in the absence and presence of inhibitor for 24 h at 25°C were examined by Atomic Force Microscopy (AFM) and recorded using an Asylum Research MFP-3D Classic AFM appliance.

3. Computational details

3.1. Quantum chemical calculations

The quantum chemical study is performed using density function theory (DFT) method, the Becke three-parameter hybrid functional together and the Lee–Yang–Paar correlation functional (B3LYP) with a 6-31G (d, p) basis set using Gaussian 09 program package was chosen for all the calculations [27-28].

E_{HOMO} and E_{LUMO} energies (highest occupied molecular orbital energy and lowest unoccupied molecular orbital energy) are used to calculate all the quantum chemical parameters such as energy gap (ΔE_{GAP}), Hardness (η), Softness (σ), Electrophilicity index(ω), Electronegativity (χ) and fraction of transferred electrons(ΔN), [29,30] these are calculated according to the following equations respectively.

$$\eta = \frac{E_{LUMO} - E_{HOMO}}{2} \qquad (7)$$

$$\sigma = \frac{1}{\eta} \qquad (8)$$

$$\omega = \frac{x^2}{2\eta} \qquad (9)$$

$$\chi = \frac{-(E_{HOMO} + E_{HOMO})}{2} \qquad (10)$$

$$\Delta N = \frac{\chi_{Fe} - \chi_{inh}}{[2(\eta_{Fe} + \eta_{inh})]} \qquad (11)$$

Where

χ_{Fe} and χ_{inh}: are the absolute electronegativity of Fe and inhibitor molecule respectively. η_{Fe} and η_{inh} : are the absolute hardness of metal and the inhibitor molecule, respectively. A value of 7.0 eV is used for χ_{Fe}, while η_{Fe} is taken as 0 for the calculation of the fraction of transferred electrons [31].

The previous parameters are very important to understand the chemical reactivity of the synthesized compound.

3.2. Molecular dynamics (MD) simulations

The simulations were carried with periodic boundary conditions in Materials Studio 7.0 (from Accelrys. Inc) [32] using the force field. Fe (110) surface was chosen for the simulation study. The simulation was carried out in a simulation box with the following dimensions (17.20 ×22.93×22.93 A˚). The iron slab, the water slab comprising the investigated inhibitor and a vacuum layer were included in the simulation box. The Fe (100) surface and the molecular structure of the inhibitor in gas phase was first optimized to minimum energy. The temperature was performed at 298 K. NVT set, (constant number of atoms, constant-volume, constant-

temperature) with a time step of 0.1 fs and simulation time of 50 ps using the COMPASS (condensed phase optimized molecular potentials for atomistic simulation studies).The following equation is used to determine the interaction energy ($E_{\text{interaction}}$) between the inhibitor and Fe (110) surface.

$$\mathrm{E_{interaction}} = \mathrm{E_{total}} - \mathrm{E_{Fe+H_2O}} - \mathrm{E_{inh}} \qquad (12)$$

Where $\mathrm{E_{total}}$ is the total energy of mild steel and inhibitor molecules, $\mathrm{E_{Fe+H_2O}}$ is the energy of iron surface simultaneously with H_2O molecules and $\mathrm{E_{inh}}$ represent the total energy inhibitor. The binding energy ($\mathrm{E_{binding}}$) of the inhibitor is the negative value of the interaction energy.

$$\mathrm{E_{binding}} = -\mathrm{E_{interaction}} (13)$$

4. Results and discussion

4.1. Weight loss results

The effect of addition of the inhibitor **TPP**, at different concentrations on the corrosion of mild steel at different immersion times in 1M HCl solution was studied by gravimetric measuring. A variation of the inhibition efficiency with concentrations of the inhibitor and various weight loss is shown in Fig. 2 the values deduced for θ and $\eta_w\%$ are summarized in Table 1.Data in Table 1 shows that the corrosion rate A decreases with the increase in concentration of the inhibitor; consequently, the surface coverage (θ) and inhibition efficiency $\eta_w\%$ are increased with the increase of the concentration of the inhibitor. Which might be due to the increase adsorption of the inhibitor TPP at the metal / solution interface as their concentration increases [33]. The adsorbed layer from the inhibitor acts as an isolation between the steel and the aggressive medium and hence delays the acidic attack [34, 35]. This type of corrosion inhibitor is increased for a long time however, the inhibitor delays the corrosion at a reduced time.

4.2. Potentiodynamic polarization curve

Fig.3 show the polarization curve for mild steel XC48 immersed in 1 m HCl in the absence and presence of different concentrations of inhibitor (TPP). The principal electrochemical parameters of corrosion extracted from polarization such as corrosion potential (E_{corr}), corrosion current density (Icorr), anodic and cathodic Tafel slopes, polarization resistance (R_P), surface coverage(θ) and inhibition efficiency (E_P) are given in Table 2. It is clear that the values of both cathodic (βc) and anodic (βa) Tafel constants are strongly changed in the presences of the inhibitor (TPP)**.** This confirms the mixed type inhibition action of the inhibitor (TPP) without changing the anodic dissolution of the metal and the cathodic evolution of hydrogen [36].

Furthermore, a slight change occurs in i_{corr} value with increasing the concentration of the inhibitor, which indicates a delay in the corrosion process [37] add to that, the maximum value of the inhibition efficiency (E_P) 51.11% at 0.075Mm. This result indicates that the inhibition activity of the studied molecule (TPP) can be related to adsorption on the metal surface to form a barrier film .This behavior leading therefore to the reduction of the anodic mild steel dissolution and the delay of the cathodic hydrogen reaction.

4.3. Electrochemical Impedance Spectroscopic Studies

The Nyquist diagrams obtained of XC48 mild steel in 1 M HCl in the absence and presence of the inhibitor (TPP) at different concentrations at 25°C are show in Fig 4. According to Nyquist diagrams, comparing between the semicircle identical forms of the mild steel shows that the real axis intercept at low frequencies in the presence of inhibitor is bigger than that in the absence of the inhibitor (blank) and increases as the same time as the concentration. This shows that no significant modification in the corrosion mechanism arises as a consequence of the inhibitor presence [38]. In effect, such phenomenon is usually attributed to the frequency dispersal which is assigned to the surface heterogeneity generated from the roughness of the surface and chemical content of mild steel [39]. Furthermore, the addition of an inhibitor increases the values of charge transfer resistance (Rct) is due to the formation of a protective film on the metal/solution interface [40]. And reduces the double layer capacitance (C_{dl}). All this is due to the reduction in local dielectric constant and/or an increment in the thickness of the electrical double layer. The phenomenon proposed that the inhibitor molecule function by the adsorption at the metal surface. Thus, the change in C_{dl} is due to the gradual replacement of the water molecule by the adsorption of the inhibitor molecule on the metal surface, decreasing the magnitude of metal dissolution [41].

The value of inhibition efficiency (E_R%) increases with the concentrations of inhibitor (TPP) and maximum efficiency (30.67%) reached at 0.075 Mm of the inhibitor for 1h, the results are summarized in Table 3.

In general, the efficiency of an organic substance as an inhibitor for metallic corrosion depend on the structure and the concentration of the inhibitor, the nature of the metal and other experimental conditions, such as the temperature of the medium [20,42].

4.4. Atomic force microscopy (AFM) studies

Fig. 5 represents the AFM surface morphology of the mild steel immersed in 1M HCl for 24 h solutions without and with the optimum concentration of the inhibitor was taken in 2D and 3D

to confirm the formation of a protective layer on the mild steel surface. It can be seen from the AFM micrograph of the mild steel (Fig.5a) in the absence of the inhibitor (Fig. 5b) that the surface showed a very irregular morphology with highly corroded and damaged surface due to corrosive attack of acid. On the other hand, in the presence of optimum concentration 0,075mM of the inhibitor (Fig. 5c), the corrosion product on the corrosion product on the surface of the metal was diminished and the surface became smoother.

The calculated surface roughness (given in table 4) of mild steel in 1 M HCl without the inhibitor (187.456 nm) was higher than that of the mild steel (7.310 nm). But in the presence of the inhibitor the value roughness was reduced to (47.051 nm) and this reduction, which confirms the formation protective surface layer by the inhibitor and corrosion rate is reduced.

4.5. Computational study

4.5.1. Quantum chemical calculations

The optimized molecular structure of the inhibitor (TPP) calculated using B3LYP/6- 31G (d, p) method of the most stable form is shown in Fig. 6. The literature shows that the adsorption of the inhibitor on the metal surface can be placed on the basis of donor–acceptor interactions between the π-electrons of the heterocyclic structure and the vacant d-orbital of the metal surface atoms. The electron acceptor distribution in the lowest unoccupied molecular orbital (LUMO) and the electron donor distribution in the highest occupied molecular orbital (HOMO) are shown in Fig.7.

Lately, quantum chemical calculations were largely used in corrosion inhibition investigations. Especially since they seem to be effective in the study of corrosion inhibition mechanisms of organic compounds [43, 44], the effectiveness of an inhibitor can be attached to some quantum chemical parameters such as: energy gap ($\Delta E_{GAP} = E_{LUMO} - E_{HOMO}$), the dipole moment (μ), and Mullikan charges on the backbone atoms which were determined by optimization and they can be related to the metal-inhibitor interactions [45]. The obtained values of the quantum chemical parameters for the investigated inhibitor are listed in Table 5.

From Fig. 7 and Table 5, we can notice that the E_{HOMO} is found to reside on the pyridine ring and heteroatoms for the studied compound and the higher value of E_{HOMO} indicates the tendency of electron transfer to an appropriate acceptor molecule which facilitates the adsorption of the inhibitor on the metal surface by influencing the electron transfer processes through the adsorbed layer [46, 47]. Moreover, the lower value of E_{LUMO}, the easier is the acceptance of electrons from the d orbital of the metal [48]. On an other hand, the value of ΔE_{GAP} provides a measure for the stability of the formed complex on the metal surface. In principle, a decrease

in the energy gap leads to easier polarization of the molecule, greater adsorption on the surface and improved the inhibition efficiency of the inhibitor [49, 50].

Several researchers have shown that the dipole moment is resultant to the polarity of an inhibitor and the elevated values of μ are answerable for great inhibition effectiveness [51, 52]. Table 5 shows that the high value of the dipole moment acquired and the low energy gap causes electron transfer from the molecule to the surface and this takes place during adsorption on the mild steel surface.

ΔN means that the fraction of transferred electrons from the inhibitor molecule to the mild steel surface and indicates the capability of the inhibitor to donate electrons. The literature shows that a value of $\Delta N < 3.6$, the inhibition effectiveness raises the electrons donating capability at the metal surface [53].

4.5.2. Molecular electrostatic potential surfaces (MEP)

The molecular electrostatic potential map (MEP) which demonstrates molecular size, shape as well as charge distribution of the compound to find the active sites responsible for electrophilic and nucleophilic attacks is a powerful tool in the study of interaction of a molecular system with its surroundings. Furthermore, MEP is related to the electronic density. Fig. 8 illustrates the map of the studied inhibitor represented by different colors. The yellow zones of the MEP represent the negative potential related to electrophilic reactivity, while the blue color represents the positive zones related to nucleophilic reactivity.

The region of the phosphonate groups is highly negatively charged (fig.8, table.6) correspond of atom oxygen obtained with Milliken charge ware located on O32, O33,O34,O36,O37,O38,O40,O41,O42, whereas positive potentials are presented at hydrogen atoms. It is clear from the Table.6 that the nitrogen atom and some carbon of TACN and pyridine of the inhibitor have negative charges, which are probably the active adsorptive sites.

4.4.3. MD simulations

The objective of this study is to find the nearer inhibitor molecule to Fe (110) surface. MD simulations were performed on a system comprising TPP molecule and iron surface in a vacuum slab (Fig. 9). From Fig. 9 we can see that the investigated inhibitor is adsorbed nearly parallel to the metal surface, this adsorption on the Fe (110) surface through oxygen, nitrogen and the pyridine rings present in the inhibitor, which leads to the formation of coordinate bonds (chemical interactions) [54]. The calculated values of the interaction and the binding energies are given in Table 7.

Conclusion

From the above results, we can deduce the following conclusions:

- ✓ The new compound TPP treated as a corrosion inhibitor in 1 M HCl in the mild steel.
- ✓ The gravimetric measurements showed that the inhibition efficiency increases with the inhibitor at different concentration and immersion times.
- ✓ The potentiodynamic polarization showed that the TPP acts as a mixed type inhibitor. EIS results reveal that the presence of the inhibitor molecules increases in the charge transfer resistance values while reducing the double layer capacitance values.
- ✓ The atomic force microscopy (AFM) showed that the surface roughness decreases in the presence of TPP, due to establishment of a protective surface
- ✓ The quantum chemical study shows that the nitrogen and oxygen atoms in the inhibitor molecule are the main active sites that result in adsorption of TPP on the mild steel surface.
- ✓ The binding energy calculated by the MD method was also in accordance with the experimental results, and the binding energy of TPP was the highest.

References

[1] M. Shymala, P.K. Kasthuri, The inhibitory action of the extracts of Adathodavasica, Ecliptaalba, and Centellaasiatica on the corrosion of mild steel in hydrochloric acid medium: a comparative study, Int. J. Corros. (2012) 1–13.

[2] L.R. Chauhan, G. Gunasekauran, Corrosion inhibition of mild steel by plant extract in dilute HCl medium, Corros. Sci. 49 (2007) 1143–1161.

[3] S.S. Shivakumar, K.N.S. Mohana, Ziziphusmauritiana leaves extracts as corrosion inhibitor for mild steel in H2SO4 and HCl solutions, Eur. J. Chem. 3 (2012) 426–432.
[4] M.A. Quraishi, A. Singh, V.K. Singh, D.K. Yadav, A.K. Singh, Green approach to corrosion inhibition of mild steel in hydrochloric acid and sulphuric acid solutions by the extract of Murrayakoenigii leaves, Mater. Chem. Phys. 122 (2010) 114–122.
[5] G. Avci, Inhibitor effect of N,N-methylenediacrylamide on corrosion behavior of mild steel in 0.5 M HCl, Mater. Chem. Phys. 112 (2008) 234–238.
[6] E.S. Meresht, T.S. Farahani, J. Neshati, 2-Butyne-1,4-diol as anovel corrosion inhibitor for API X65 steel pipeline in carbon-ate/bicarbonate solution, Corros. Sci. 54 (2012) 36–44.
[7] M. Heydari, M. Javidi, Corrosion inhibition and adsorption behaviour of an amido-imidazoline derivative on API 5L X52 steel in CO2-saturated solution and synergistic effect of iodide ions, Corros. Sci. 61 (2012) 148–155.
[8] X. Jiang, Y.G. Zheng, W. Ke, Effect of flow velocity and entrained sand on inhibition performances of two inhibitors for CO2 corrosion of N80 steel in 3% NaCl solution, Corros. Sci. 47 (2005) 2636–2658.
[9] A.Garnica-Rodriguez, J. Genesca, J. Mendoza-Flores, R. Duran-Romero, Electrochemical evaluation of aminotriazole corrosion inhibitor under flow conditions, J. Appl. Electrochem. 39 (2009) 1809–1819.
[10] P.C. Okafor, X. Liu, Y.G. Zheng, Corrosion inhibition of mild steel by ethylamino imidazoline derivative in CO2-saturated solution, Corros. Sci. 51 (2009) 761– 768.
[11] A.A. Mazhar, W.A. Badaway, M.M. Abou-Romia. Impedance studies of corrosion resistance of aluminium in chloride media. Surf.Coat.Techol. 29 (1986) 335-345.
[12] A. Zarrouk, B. Hammouti, H. Zarrok, R. Salghi, A. Dafali, Lh.Bazzi, L. Bammou, S.S. Al-Deyab, Electrochemical impedancespectroscopy and weight loss study for new pyridazine derivativeas inhibitor for copper in nitric acid, Der Pharm. Chem. 4 (2012)337–346.
[13] M. Gopiraman, N. Selvakumaran, D. Kesavan, R. Karvembu, Adsorption and corrosion inhibition behaviour of N-(phenylcarbamothioyl)benzamide on mild steel in acidic medium, Prog. Org. Coat. 73 (2012) 104–111.
[14] H. Hamani, T. Douadi, M. Al-Noaimi, S. Issaadi, D. Daoud, S. Chafaa. Electro-chemical and quantum chemical studies of some azomethine compounds as corrosion inhibitors for mild steel in 1 M hydrochloric acid.CorrosSci 88 (2014) 234–245 .
[15] S.L. Granese, B.M. Rosales, C. Oviedo, J.O. Zerbino. The inhibition action of hete-rocyclic nitrogen organic compounds on Fe and steel in HCl media.Corrosion Sci 33(1992)1439–53.
[16] El Ashry E , El Nemr A , Essawy S , Ragab S . Corrosion inhibitors part V: QSAR of benzimidazole and 2-substituted derivatives as corrosion inhibitors by using the quantum chemical parameters. Prog Org Coat 61 (2008)11–20.
[17] M. Djenane, S. Chafaa, N. Chafai, R. Kerkour, A. Hellal. Synthesis, spectral properties and corrosion inhibition efficiency of new ethyl hydrogen [(methoxyphenyl)(methylamino) methyl] phosphonate derivatives: Experimental and theoretical investigation. Journal of Molecular Structure. 1175 (2018) 398−413.
[18] M.R. Laamari, J. Benzakour, F. Berrekhis, A. Derja, D. Villemin. Adsorption and corrosion inhibition of mild steel in hydrochloric acid medium by hexamethylenediamine tetra(methylene phosphonic acid) Arabian Journal of Chemistry 9 (2016) 245–251
[19] H.Amar,J.Benzakour,A.Derja,D.Villemin,B.Moreau,T.Braisaz.Piperidin-1-yl-phosphonic acid and (4-phosphono-piperazin-1-yl) phosphonic acid: A new class of iron corrosion inhibitors in sodium chloride 3% media. Applied Surface Science 252 (2006) 6162-6172

[20] K. Benbouguerra, S. Chafaa, N. Chafai, M. Mehri, O. Moumeni, A. Hellal. Synthesis, spectroscopic characterization and a comparative study of the corrosion inhibitive efficiency of an α-aminophosphonate and Schiff base derivatives: Experimental and theoretical investigations. Journal of Molecular Structure. 1157 (2018) 165−176.

[21] M.R. Laamari, J. Benzakour, F. Berrekhis, M. Bakasse, D. Villemin. Investigation of the effect of piperidin-1-ylphosphonic acid on corrosion of iron in sulfuric acid.Arabian Journal of Chemistry 9 (2016) 1218–1224

[22] J.Salaam,L.Tabti,S.Bahamyirou,A.Lecointre,O.H.Alba,O.Jeannin,F.Camerel,S. Cianférani,E.Bentouhami, A.M. Nonat,and L.J. Charbonnière. Formation of Mono- and Polynuclear Luminescent Lanthanide Complexes based on the Coordination of PreorganizedPhosphonated Pyridines Inorg. Chem. 57 (2018) 6095−6106

[23] A. A. Farag, M.R. Noor El-Din, The adsorption and corrosion inhibition of some nonionic surfactants on API X65 steel surface in hydrochloric acid, Corros. Sci. 64 (2012) 174–183.

[24] D.K. Yadav, M.A. Quraishi, B. Maiti, Inhibition effect of some benzylidenes on mild steel in 1 M HCl: an experimental and theoretical correlation. Corros. Sci. 55 (2012) 254–266.

[25] Z Tao,S Zhang, WLi, B Hou.Corrosion inhibition of mild steel in acidic solution by some oxo-triazole derivatives.Corros.Sci.51 (2009) 2588-95.

[26] M Shahin, S Bilgic, H Yilmaz. The inhibition effects of some cyclic nitrogen compoundson the corrosion of the steel in NaCl medium. Appl. Surf. Sci. 195(2003) 1–7.

[27] A.D.Becke, A new mixing of Hartree–Fock and local density-functional theories. J.Chem.Phys 98 (1993)1372-1377.

[28] H.B. Schlegel, G.E. Scuseria, M.A. Robb, J.R. Cheeseman, G. Scalmani, V. Barone, B. Mennucci, G.A. Petersson, H. Nakatsuji, M. Caricato, X. Li, H.P. Hratchian, A.F. Izmaylov, J. Bloino, G. Zheng, J.L. Sonnenberg, M. Hada, M. Ehara, K. Toyota, R. Fukuda, J. Hasegawa, M. Ishida, T. Nakajima, Y. Honda, O. Kitao, H. Nakai, T. Vreven, J.A. Montgomery Jr., J.E. Peralta, F. Ogliaro, M. Bearpark, J.J. Heyd, E. Brothers, K.N. Kudin, V.N. Staroverov, R. Kobayashi, J. Normand, K. Raghavachari, A. Rendell, J.C. Burant, S.S. Iyengar, J. Tomasi, M. Cossi, N. Rega, J.M. Millam, M. Klene, J.E. Knox, J.B. Cross, V. Bakken, C. Adamo, J. Jaramillo, R. Gomperts, R.E. Stratmann, O. Yazyev, A.J. Austin, R. Cammi, C. Pomelli, J.W. Ochterski, R.L. Martin, K. Morokuma, V.G. Zakrzewski, G.A. Voth, P. Salvador, J.J. Dannenberg, S. Dapprich, A.D. Daniels, O. Farkas, J.B. Foresman, J.V. Ortiz, J. Cioslowski, D.J. Fox, Gaussian 09, Revision A.02, Gaussian, Inc., Wallingford, CT, 2009.

[29] B. Ramaganthan, M. Gopiraman, L.O. Olasunkanmi, M.M. Kabanda, S. Yesudass, I. Bahadur, A.S. Adekunle, I.B. Obot, E.E. Ebenso, Synthesized photo-cross-linking chalcones as novel corrosion inhibitors for mild steel in acidic medium: experimental, quantum chemical and Monte Carlo simulation studies, RSC Adv. 5 (2015) 76675–76688.

[30] E.E. Oguzie, C.B. Adindu, C.K. Enenebeaku, C.E. Ogukwe,M.A. Chidiebere, K.L. Oguzie, Natural products for materials protection: mechanism of corrosion inhibition of mild steel by acid extracts of Piper guineense, J. Phys. Chem. C 116 (2012) 13603–13615.

[31] V.S. Sastri, J.R. Perumareddi . Molecular orbital theoretical studies of some or- ganic corrosion inhibitors.Corrosion 53 (1997) 617–629.

[32] Materials studio, 7.0 San Diego, CA: Accelrys Inc.; 2013.

[33] I.B. Obot, N.O. Obi-Egbedi. Anti-corrosive properties of xanthone on mild steel corrosion in sulphuric acid: experimental and theoretical investigations, Curr. Appl. Phys. 11 (2011) 382–392.
[34] A.K. Maayta, N.A.F. Al-Rawashdeh. Inhibition of acidic corrosion of pure aluminum by some organic compounds.Corros. Sci. 46 (2004) 1129-1140
[35] J. Aljourani, K. Raeissi, M.A. Golozar. Benzimidazole and its derivatives as corrosion inhibitors for mild steel in 1M HCl solution. Corros. Sci. 51 (2009) 1836-1843
[36] C.Cao. On Electrochemical technique for interface inhibitor research.Corrs.Sci.38 (1996) 2073-2082.
[37] I.B .Obot, N.O. Obi-Egbedi, N.W. Odozi. Acenaphtho[1,2-b] quinoxaline as a novel corrosion inhibitor for mild steel in 0.5M H_2SO_4. Corros. Sci. 52(2010) 923–926.
[38] N.Labjar, M.Lebrini, F.Bentiss, N.E.Chihib, S.El Hadjjaji, C.Jama. Corrosion inhibition of mild steel and antibacterial proprieties of aminotris(methyl nephosnic) acid,Mater.Chem.Phys.119 (2010) 330-336.
[39] F.Bentiss, M. Lebrini, M. Lagrenee, Thermodynamic characterization of metal dissolution and inhibitor adsorption processes in mild steel/2,5-bis(n-thienyl)- 1,3,4-thiadiazoles/hydrochloric acid system, Corros. Sci. 47 (2005) 2915–2931.
[40] W. Li, Q. He, S. Zhang, C. Pei, B. Hou, Some new triazole derivatives as inhibitors for mild steel corrosion in acidic medium J. Appl. Electrochem. 38 (2008) 289–295.
[41] C.M. Goulart, A. Esteves-Souza, C.A. Martinez-Huitle, C.J.F. Rodrigues, M.A.M. Maciel, A. Echevarria, Experimental and theoretical evaluation of semicarbazones and thiosemicarbazones as organic corrosion inhibitors, Corros. Sci. 67 (2013) 281–291.
[42] R. Hasanov, M. Sadıkoğlu, S. Bilgic, Electrochemical and quantum chemical studies of some Schiff bases on the corrosion of steel in H_2SO_4 solution, Appl. Surf. Sci. 253 (2007) 3913–3921.
[43] G. Gece .The use of quantum chemical methods in corrosion inhibitor studies.CorrosSci 50 (2008) 2981–2992.
[44] E. Jamalizadeh, S.M.A. Hosseini, A.H.Jafari. Quantum chemical studies on corrosion inhibition of some lactones on mild steel in acid media.CorrosSci 51 (2009) 1428–1435.
[45] K. F. Khaled .Electrochemical investigation and modeling of corrosion inhibition of aluminum in molar nitric acid using some sulphur-containing amines.CorrosSci 52 (2010) 2905–2916.
[46] I. Lukovits, K. Pálfi, I. Bakó, E. Kálmán. LKP model of the inhibition mechanism of thiourea compounds. Corrosion 53 (1997) 915–919.
[47] A.Y. Musa, A.A.H. Kadhum, A.B. Mohamad, A.A. Rahoma, H. Mesmari, Electrochemical and quantum chemical calculations on 4,4- dimethyloxazolidine-2-thione as inhibitor for mild steel corrosion in hydrochloric acid, J. Mol. Struct. 969 (2010) 233–237.
[48] M. Finšgar, A. Lesar, A. Kokalj, I. Milošev, A comparative electrochemical and quantum chemical calculation study of BTAH and BTAOH as copper corrosion inhibitors in near neutral chloride solution, Electrochim. Acta 53 (28) (2008) 8287–8297.
[49] D. Zhang, Z. An, Q. Pan, L. Gao, G. Zhou, Comparative study of bis-piperidiniummethyl-urea and mono-piperidiniummethyl-urea as volatile corrosion inhibitors for mild steel, Corrosion Sci. 48 (2006) 1437-1448.
[50] A.S. Fouda, A.S. Ellithy. Inhibition effect of 4-phenylthiazole derivatives on corrosion of 304L stainless steel in HCl solution.Corros. Sci. 51 (2009) 868–875.
[51] R.M. Issa, M.K. Awad, F.M. Atlam, Quantum chemical studies on the inhibition of corrosion of copper surface by substituted uracils, Appl. Surf. Sci. 255 (2008) 2433-2441.

[52] M. Lashkari, M.R. Arshadi, DFT studies of pyridine corrosion inhibitors in electrical double layer: solvent, substrate, and electric field effects, Chem.Phys. 299 (2004) 131-137.
[53] I. Lukovits, E. Kálmán, F. Zucchi, Corrosion inhibitors-correlation between electronic structure and efficiency, Corrosion 57 (2001) 3-8.
[54] N. Chafai, S. Chafaa, K. Benbouguerra, D. Daoud, A. Hellal, M. Mehri. Synthesis, characterization and the inhibition activity of a new αaminophosphonic derivative on the corrosion of XC48 mild steel in 0.5 M H_2SO_4: Experimental and theoretical studies..Journal of the Taiwan Institute of Chemical Engineers 70 (2017) 331–344

Table Captions

Table 1

Gravimetric results of mild steel at different immersion times in 1M HCl without and with the addition of the inhibitor at 25°C.

Table 2

Electrochemical corrosion parameters of mild steel in the absence and presence of various concentrations of inhibitor (TPP) in 1M HCl.

Table 3

Electrochemical impedance parameters for mild steel in 1 M HCl containing different concentrations of inhibitor (TPP).

Table 4

Table 4 AFM data obtained of mild steel in 1 M HCl immersed in inhibited and uninhibited at 298 K.

Table 5

Calculated quantum chemical parameters of the investigated inhibitor (TPP).

Table 6

Obtained Mullikan atomic charges of the inhibitor (TPP).

Table 7

Interaction and binding energies between the inhibitor molecules (TPP) and Fe (100) surface.

Figure Captions

Figure 1. The chemical structure of the inhibitor **TPP.**

Figure 2. Variation of the corrosion rate (■) and the inhibition efficiency (▲) with various concentration of inhibitor (TPP).

Figure 3. Tafel polarization curves for the corrosion of mild steel XC48 in 1 M HCl with and without various concentrations of the inhibitor at 25°C.

Figure 4. Nyquist plots for the mild steel XC48 in 1 M HCl solution with different concentrations of the inhibitor (TPP).

Figure 5. AFM images 2D (on the Left) and 3D (on the Right), mild steel surface ; (XC48) polished mild steel, mild steel in 1 M HCl , mild steel after immersion in 1 M HCl in presence of 0.075m M of inhibitor(TPP).

Figure 6. Optimized molecular structure of inhibitor **TPP.**

Figure 7. The frontier molecular orbital density distributions for inhibitor (TPP)**.**

Figure 8. Molecular electrostatic potential of inhibitor (TPP)**.**

Figure 9. Equilibrium configuration of the adsorbed molecule on the Fe (110) surface vacuum slab: (a) top view, (b): side view.

Table 1

Gravimetric results of mild steel at different immersion times in 1M HCl without and with the addition of the inhibitor at 25°C (S=3.14cm^2).

Concentration / time (mM)		Δm (mg)	A (mg/cm^{2}h)	Θ	η_w (%)
Blanc		476.3	15.16	--	--
0.010		288.1	9.17	0.40	40
0.025	**10** Hours	240.7	7.66	0.48	48
0.050		190.6	6.07	0.60	60
0.075		150.2	4.78	0.68	68
Blanc		476.3	7.58	--	--
0.010		252.8	4.03	0.47	47
0.025	**20** Hours	211.3	3.36	0.55	55
0.050		145.2	2.31	0.70	70
0.075		101.5	1.62	0.78	78
Blanc		476.3	5.04	--	--
0.010		232.5	2.46	0.51	51
0.025	**30** Hours	190.8	2.01	0.60	60
0.050		120.5	1.27	0.75	75
0.075		082.6	0.87	0.83	83
Blanc		476.3	3.792	--	--
0.010		220.0	1.751	0.54	54
0.025	**40** Hours	157.1	1.250	0.67	67
0.050		095.1	0.757	0.80	80
0.075		051.9	0.413	0.90	90

Table 2

Electrochemical corrosion parameters of mild steel in the absence and presence of various concentrations of inhibitor (TPP) in 1M HCl 25°C / 1h.

Concentration (mM)	$-E_{corr}$ (mV/ECS)	$-\beta_c$ (mV/dec)	β_a (mV/dec)	i_{corr} ($\mu A/cm^2$)	R_p (Ωcm^2)	E_P (%)	θ
Blanc	463	150.5	119.1	0.090	246.6	--	--
0.010	458	129.3	104.2	0.074	287.2	17.77	0.17
0.025	454	114.4	139.6	0.067	319.5	25.55	0.25
0.050	451	123.2	102.2	0.062	328.4	31.11	0.31
0.075	446	102.6	112.5	0.044	338.1	51.11	0.51

Table 3
Electrochemical impedance parameters for mild steel in 1M HCl containing different concentrations of inhibitor (TPP) 25°C/1h.

Concentration (mM)	R_s (Ω cm^2)	R_{ct} (Ω cm^2)	C_{dl} ($\mu F/cm^{-2}$)	E_R (%)
Blanc	2.54	196.4	293.2	--
0.010	2.63	244.5	172.0	19.67
0.025	3.02	256.1	153.5	23.31
0.050	2.68	264.6	151.5	25.77
0.075	3.10	283.3	95.4	30.67

Table 4

AFM data obtained of mild steel in 1 M HCl immersed in inhibited and uninhibited at 298 K.

AFM data	Mild steel	1 M HCl Blank	0,075 mM
roughness (nm)	7.310	187.456	47.051

Table 5
Calculated quantum chemical parameters of the investigated inhibitor (TPP).

Quantum chemical parameter	Inhibitor**TPP**
E_{Tot} (eV)	-80660.7952822213
E_{HOMO} (eV)	-8.62955
E_{LUMO} (eV)	-5.3516653
ΔE_{GAP} (eV)	3.2778847
μ (Debye)	6.4605
η (eV)	1.6389424
Σ	0.6101495
χ (eV)	6.9906077
Ω	14.909856
ΔN	0.002865354

Table 6

Obtained Mullikan atomic charges of the inhibitor (TPP).

Atom	Mulliken Charge	Atom	Mulliken Charge	Atom	Mulliken Charge
C1	-0.4062436	N26	-0.5924872	H51	0.2832758
C2	-0.4408006	C27	0.2390047	H52	0.2668431
C3	-0.4636576	C28	-0.3732743	H53	0.2767447
N4	-0.4827192	C29	-0.3896199	H54	0.3216647
C5	-0.3685648	C30	-0.2408759	H55	0.2925512
N6	-0.4010391	P31	1.7598520	H56	0.3009605
N7	-0.4406184	O32	-0.9412391	H57	0.2999258
C8	-0.3692009	O33	-0.8002294	H58	0.3022151
C9	-0.5867098	O34	-0.7998068	H59	0.2819155
C10	-0.4273687	P35	1.7669255	H60	0.2881563
C11	0.4210028	O36	-0.9464684	H61	0.2742818
C12	-0.4881902	O37	-0.8034906	H62	0.2833459
C13	0.3961610	O38	-0.8048440	H63	0.2806907
C14	-0.4518575	P39	1.7616839	H64	0.2802377
C15	0.4137919	O40	-0.9432346	H65	0.2834756
C16	-0.3839464	O41	-0.8019828	H66	0.2733855
C17	0.2415364	O42	-0.7782755	H67	0.2800620
C18	-0.2352215	H43	0.2695002	H68	0.2740097
N19	-0.6074982	H44	0.2768180	H69	0.2839072
C20	-0.3682742	H45	0.2799293	H70	0.4849134
C21	-0.3656204	H46	0.2882830	H71	0.4837532
C22	-0.2252762	H47	0.2714893	H72	0.4844964
C23	-0.3914421	H48	0.2882618	H73	0.4839059
N24	-0.6253853	H49	0.2808502	H74	0.4845003
C25	0.2672377	H50	0.1894533	H75	0.4844648

Table 7
Interaction and binding energies between the inhibitor molecules (TPP) and Fe (100) surface.

Systems	$E_{Interaction}$ (kJ mol^{-1}	$E_{binding}$ (kJ mol^{-1})
Fe + Inhibitor	- 1071,181	1071,181

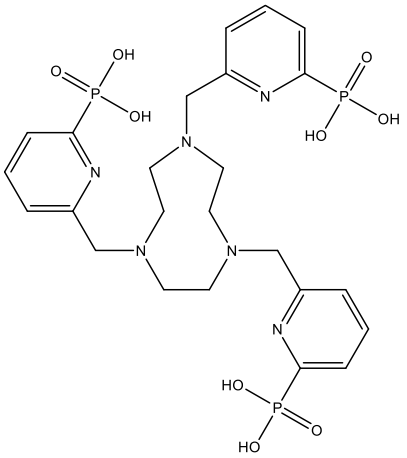

Figure 1. The chemical structure of the inhibitor TPP

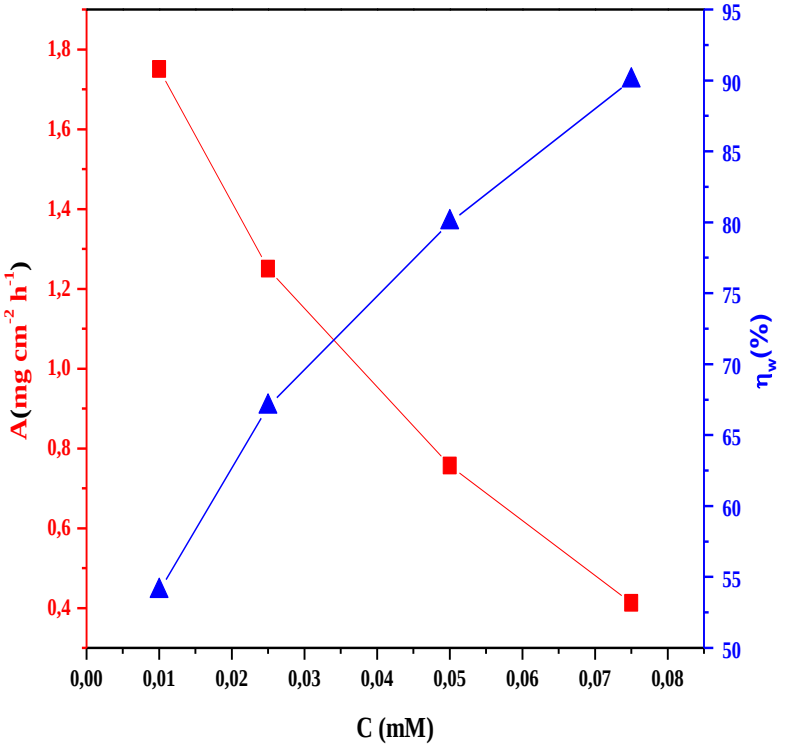

Figure 2. Variation of the corrosion rate A (■) and the inhibition efficiency η_w (▲) with various concentration of inhibitor (TPP).

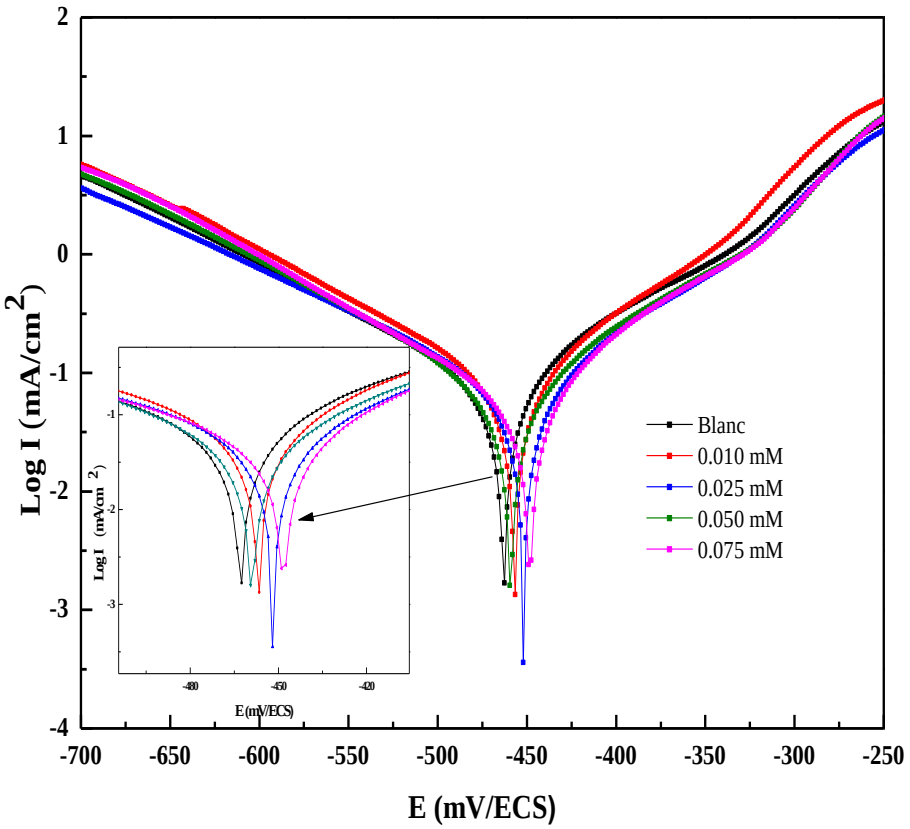

Figure 3. Tafel polarization curves for the corrosion of mild steel XC48 in 1 M HCl with and without various concentrations of the inhibitor at 25°C.

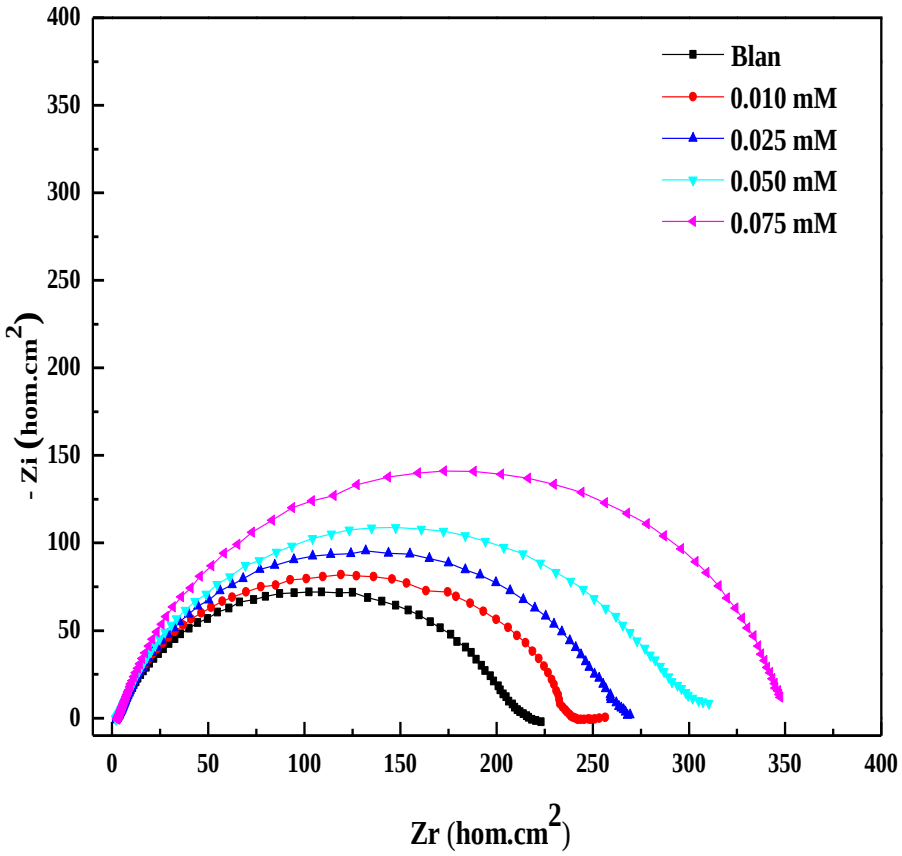

Figure 4. Nyquist plots for the mild steel XC48 in 1 M HCl solution without and with different concentrations of the inhibitor (TPP).

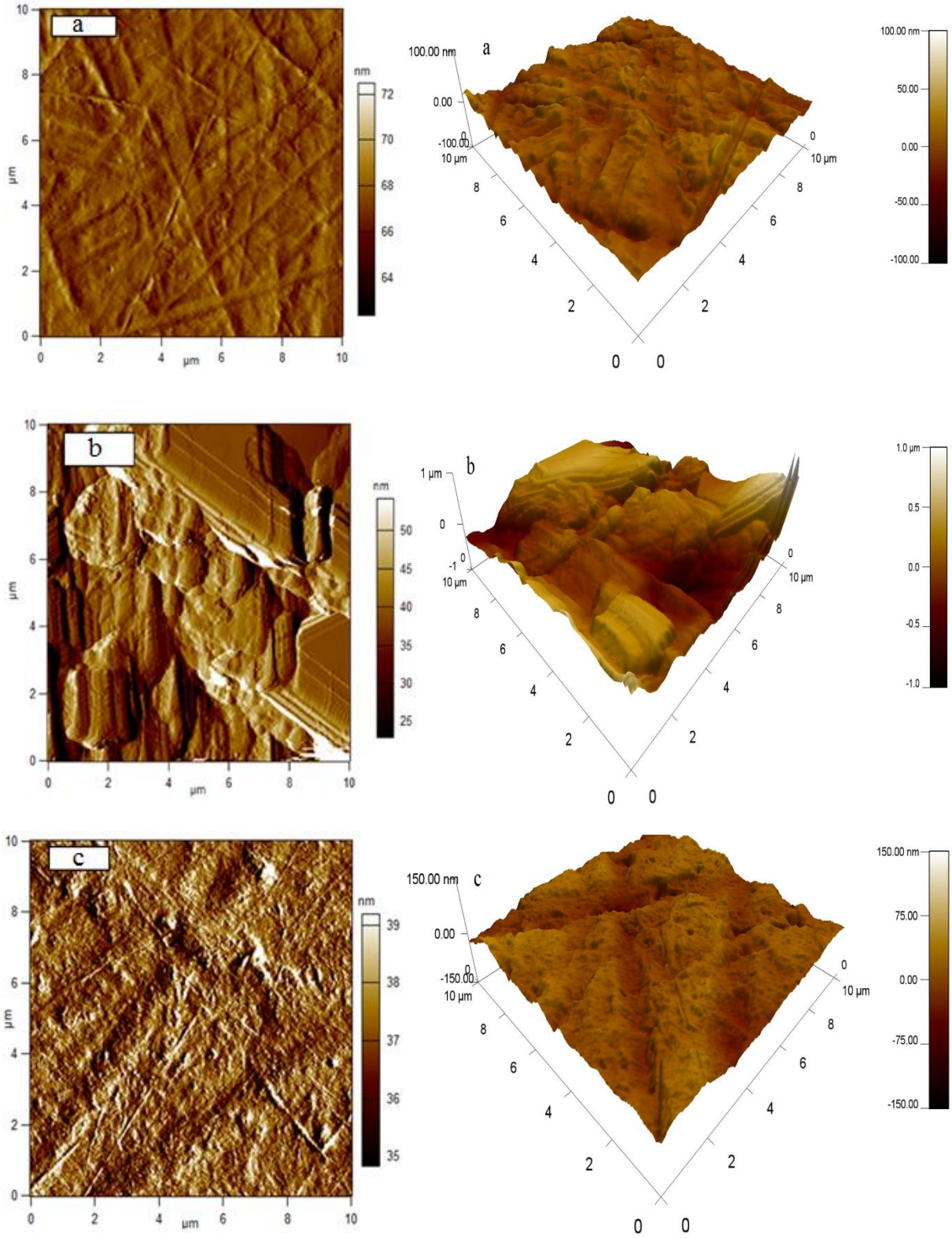

Figure 5. AFM images 2D (on the Left) and 3D (on the Right), mild steel surface ; (XC48) polished mild steel, mild steel in 1 M HCl , mild steel after immersion in 1 M HCl in presence of 0.075m M of inhibitor(TPP).

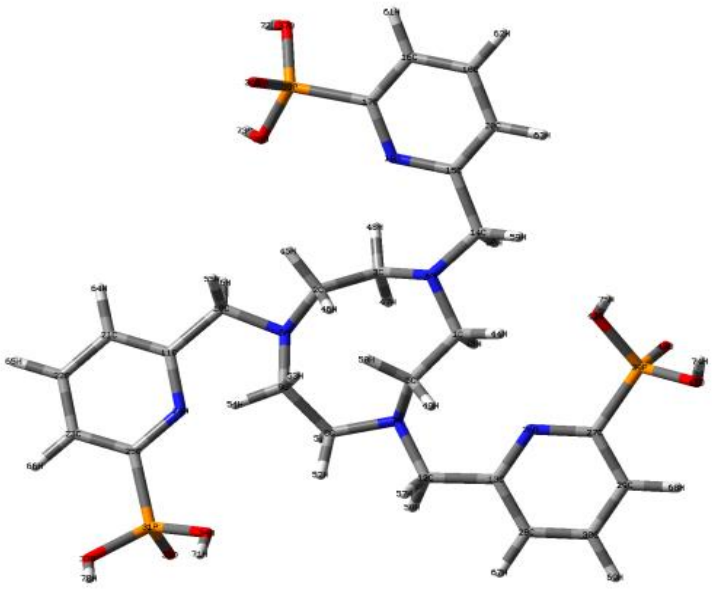

Figure 6. Optimized molecular structure of inhibitor **TPP.**

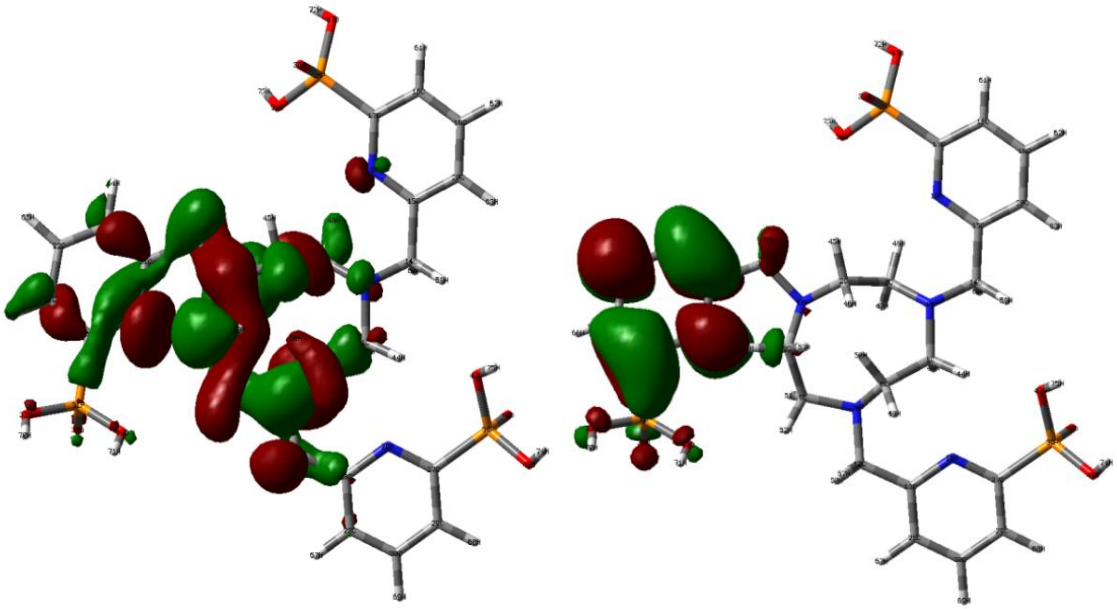

HOMO **LUMO**

Figure 7. The frontier molecular orbital density distributions for inhibitor (TPP)**.**

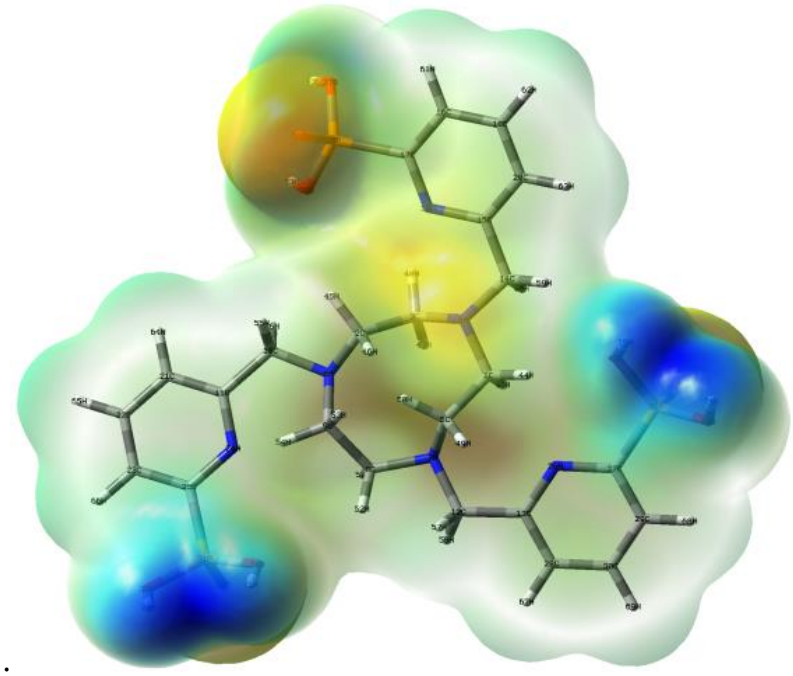

Figure 8. Molecular electrostatic potential of inhibitor (TPP)**.**

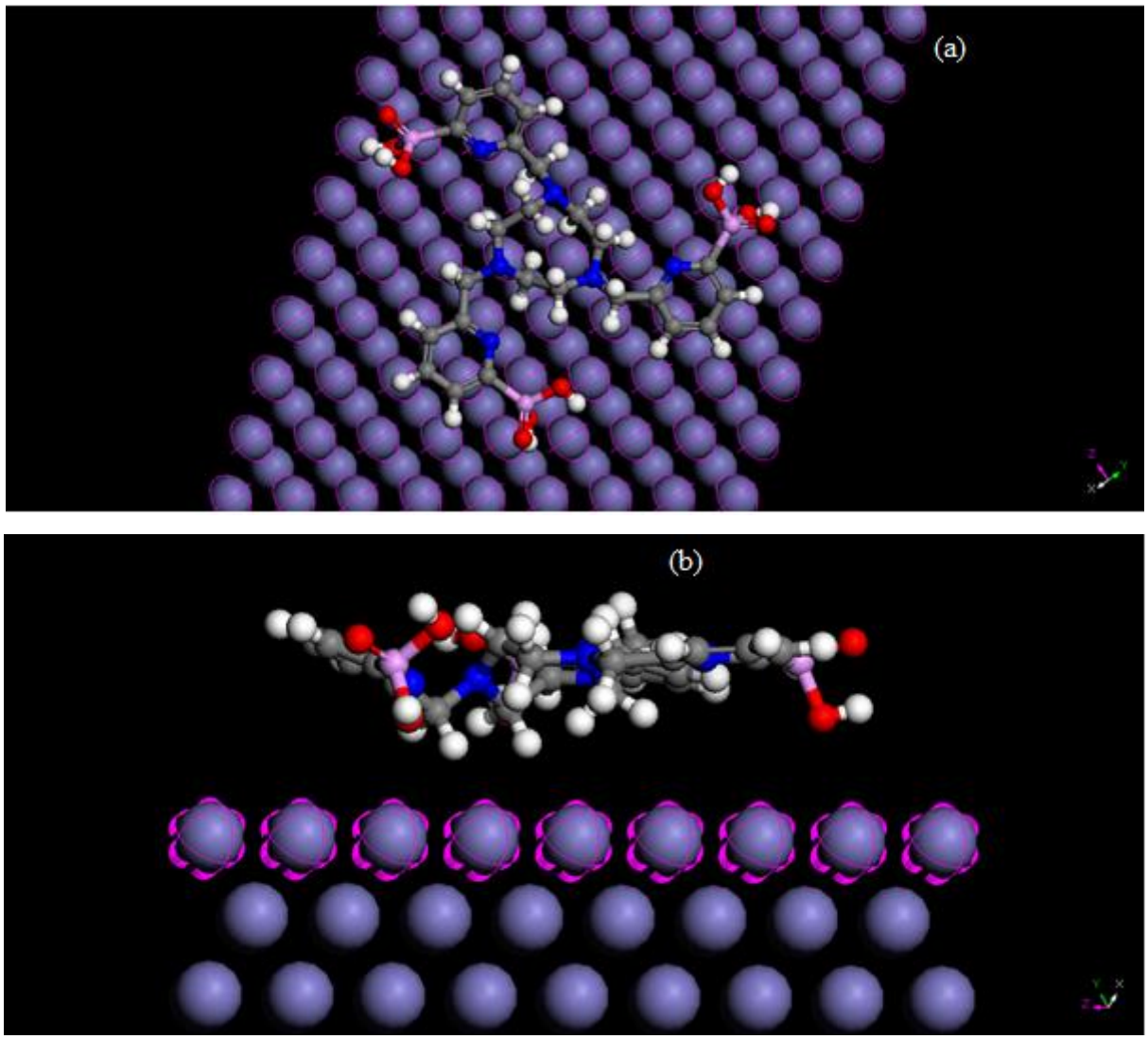

Figure 9. Equilibrium configuration of the adsorbed molecule on the Fe (110) surface vacuum slab: (a) top view, (b): side view.

Highlights:

- New organic inhibitor (1,4,7-tris[hydrogen (6-methylpyridin-2-yl) phosphonate]-1,4,7-triazacyclononane) (TPP) act as an excellent inhibitor for mild steel in 1 M HCl solution.
- The corrosion inhibition efficiency of TPP is 90% at 0.075mM (obtained from Gravimetric for 40 h) and increases with different concentration and immersion time.
- Theoretical calculations provide favorable support for the experimental data.